X-651-73-64
PREPRINT

THE NIMBUS-4 BACKSCATTER ULTRAVIOLET (BUV) ATMOSPHERIC OZONE EXPERIMENT- TWO YEARS' OPERATION

DONALD F. HEATH
CARLTON L. MATEER
ARLIN J. KRUEGER

FEBRUARY 1973

GSFC

GODDARD SPACE FLIGHT CENTER
GREENBELT, MARYLAND

THE NIMBUS-4 BACKSCATTER ULTRAVIOLET (BUV) ATMOSPHERIC OZONE EXPERIMENT-TWO YEARS' OPERATION

Donald F. Heath[1]
Carlton L. Mateer[2]
Arlin J. Krueger[1]

February 1973

[1]Goddard Space Flight Center, Greenbelt, Maryland 20771, U.S.A.
[2]Atmospheric Environment Service, 4905 Dufferin Street, Downsview, Ontario, Canada.

GODDARD SPACE FLIGHT CENTER
Greenbelt, Maryland

CONTENTS

THE NIMBUS-4 BACKSCATTER ULTRAVIOLET (BUV) ATMOSPHERIC OZONE EXPERIMENT - TWO YEARS' OPERATION

ABSTRACT

In April 1970 the Backscatter Ultraviolet (BUV) experiment was placed into orbit aboard the Nimbus-4 satellite. This double monochromator experiment measures ultraviolet terrestrial radiance at 12 discrete wavelengths between 2550 Å and 3400 Å. Approximately 100 scans covering a 230 kilometer square are made between terminator crossings on the daylight side of the earth. A colinear photometer channel with the same field of view is used to derive the Lambert reflectivity of the lower boundary of the scattering atmosphere. The extraterrestrial solar irradiance is measured at the northern terminator. The instrument has currently produced almost three years of nearly continuous data which are being used to infer the high-level ozone distribution and total ozone on a global basis. The high-level ozone data have been verified by independent coincident rocket ozone soundings, and the total ozone values show good agreement with Dobson spectrophotometer determinations as well as those made with the Infrared Interferometer Spectrometer also on Nimbus-4. An increase has been observed in equatorial radiance at 2550 Å relative to 2900 Å, which seems to indicate that the amount of ozone in the upper stratosphere is related to the 11-year solar cycle.

1. INTRODUCTION

That satellite measurements of scattered ultraviolet solar radiation from the terrestrial atmosphere could be used to deduce ozone profiles on a global basis was first suggested by Singer and Wentworth [14]. The dynamic range of this measurement is quite severe, since the radiance of the terrestrial atmosphere increases by about 10^4 from 2550 Å to 3400 Å and the linear polarization of the radiation may range from 0 percent to nearly 100 percent. Furthermore, the atmospheric albedo, (that is, atmospheric radiance/solar irradiance) must be determined within limits of error of 1 to 3 percent if reliable ozone profiles are to be inferred. Subsequent satellite applications of this technique have been reported by Rawcliffe and Elliot [13] for a photometer experiment; by Krasnopol'skiy [9], Iozenas [6], Iozenas et al. [7, 8], and Anderson et al. [1] for monochromator experiments.

On April 8, 1970, the Nimbus-4 satellite was launched into a circular polar orbit at an altitude of 1100 kilometers. The 10° retrograde orbit is sun synchronous, and every 107 minutes the three-axis stabilized satellite passes through the ascending mode near local noon. The subsatellite point crosses the equator in increments of 27° in longitude between successive passes, and reaches a maximum latitude of 80°. The Backscatter Ultraviolet experiment (BUV) is designed to measure the solar irradiance at the top of the atmosphere and the atmospheric radiance in the satellite nadir direction, thus providing data for

determination of high-level ozone profiles and total ozone amounts on a global basis, with a spatial resolution of 230 kilometers.

2. PHYSICAL BASIS

For a single-scattering model atmosphere the atmospheric radiance is

$I(\lambda,\theta) = F_0(\lambda)(3\beta_\lambda/16\pi)(1 + \cos^2\theta) \int_0^1 \exp\left[-(1 + \sec\theta)(\alpha_x X_p + \beta_\lambda P)\right]dp$ where

$F_0(\lambda)$ = extraterrestrial solar irradiance (ergs/cm^2 · sec · Å)

$I(\lambda,\theta)$ = atmospheric radiance (ergs/cm^2 · sec · Å · ster)

β_λ = atmospheric scattering coefficient (atm^{-1})

σ_λ = ozone absorption coefficient (atm · cm)$^{-1}$

X_p = amount of ozone above pressure p (atm) in atm · cm

θ = solar zenith angle

The inversion of terrestrial atmospheric radiance to obtain vertical ozone profiles is possible since atmospheric radiance at a particular wavelength originates in a moderately well-defined effective scattering layer. The central height and width of a layer is principally a function of the ozone absorption coefficient, solar zenith angle, and ozone distribution. An example of effective scattering layers is given in Figure 1 for a solar zenith angle of 60° and a total ozone amount of 336 m atm · cm. The curves are normalized to unity at the maximum. Mateer [11] provides a comprehensive discussion of inversion of ultraviolet atmospheric radiances to obtain a vertical distribution of ozone.

The basis for derivation of total ozone from the satellite observation of the atmospheric radiance in the Hartly-Huggins bands is provided by Dave and

Mateer [3]. The application of this technique in the BUV experiment has been described by Mateer, Heath, and Krueger [12]. The inference of total ozone is made from measurements at ultraviolet wavelengths which are weakly absorbed near the long-wavelength end of the ozone absorption band. The absorption must be sufficiently weak so that the solar photons have traversed the ozone layer with significant absorption and have been scattered by the troposphere and ground back into space. A wavelength pair, separated by about 200 Å to minimize scattering effects, is chosen so that one is fairly strongly absorbed while the other is only weakly absorbed by ozone. Two wavelength pairs are necessary to cover the range of solar zenith angles from 0° to 90°. The two line pairs are: (A) 3125 Å, 3312 Å, and (B) 3175 Å, 3398 Å.

The basic observation is the relative logarithmic attenuation

$$N(3125, 3312) = \log_{10} \{F_0/I\}_{3125} - \log_{10} \{F_0/I\}_{3312}$$

where

F_0 = extraterrestrial solar irradiance

I = terrestrial radiance

the total ozone is estimated by comparing the observed value of N with values which have been calculated previously for the following:

a) Solar zenith angles from 0° to 90°

b) Two lower boundary pressures of 400 mb and 1000 mb

c) Series of standard ozone profiles

d) Range of Lambertian reflectancies

This procedure minimizes computer time since a multiple scattering problem is involved.

3. INSTRUMENTATION

a. Optical

The BUV experiment is located in bay 9 of the Nimbus sensory ring. In this location the experiment views the earth in the satellite nadir direction with a 12° field of view, a square 230 kilometers on a side at the surface. At the end of a measurement cycle of 32 seconds, the subsatellite point has moved about 200 kilometers.

The instrument basically consists of a double (tandem) Ebert-Fastie spectrophotometer in conjunction with a narrow-band interference filter photometer. The spectrophotometer is designed to measure spectral intensitites at 12 wavelengths from 2555 Å to 3398 Å with a 10 Å bandpass while the interference filter photometer records a 50 Å band centered at 3800 Å. This combination of instruments measures the backscattered ultraviolet solar radiation from the daytime illuminated atmosphere, as well as the direct solar rays reflected off a diffuser plate.

The layout of the optical components of the double monochromator and interference filter photometer is shown in Figure 2. Sunlight diffusely reflected from the atmosphere enters the two systems through the optical horns. A double-Lyot type depolarizer is inserted in front of the entrance slit of the spectrophotometer in order to render its throughput independent of the state of

polarization of the incident radiation. The double monochromator is composed of two 25-cm focal length Ebert-Fastie monochromators. Light entering the entrance slit is rendered parallel by the spherical collimator mirror and is then diffracted by a 52-by-52-mm grating of 2400 grooves/mm (solid angle is 0.043 steradians). The diffracted light returns to the spherical collimating mirror, passes through the roof prism, and is imaged onto an intermediate slit. The light passing through the intermediate slit is dispersed again by the second monochromator. A field lens at the exit slit is used to image the gratings onto the photocathode of the photomultiplier. Both gratings are mounted on a common rigid shaft to eliminate wavelength tracking errors between the two monochromators. A roof prism is used to invert the image in the direction of dispersion at the intermediate slit, in order to double the dispersion by passing through the second monochromator. A slit aperture is placed in the interference filter photometer so that it will have the same field of view as the spectrophotometer. Both of the monochromator and photometer slits are aligned at 10° to the spacecraft velocity vector. When passing over the polar regions, diffuser plates are deployed in front of the spectrophotometer and the filter photometer to measure the extraterrestrial solar irradiance.

The primary reason for using a double monochromator is to obtain the desired spectral purity, that is, the elimination of scattered light, which permits one to use a high quantum efficiency (20 percent for the 12 wavelengths) photomultiplier tube with a dark current of the order of 10^{-11} amp at a gain of 10^{6}.

The instrumental scattered light contributes less than 1 percent of the atmospheric radiance signal at 2550 Å.

From an extensive ray-trace analysis, which was subsequently confirmed by experimental observations, it was found that the optical aberrations are less at the exit slit of the double monochromator than they are at the exit slit of a corresponding single monochromator. This is related to the fact that certain optical aberrations cancel as a result of the second reflection from the spherical collimating mirror in the Ebert-Fastie single monochromator. A similar cancelling of aberrations is observed in passing through the second half of the double monochromator.

The wavelength scan is accomplished by rotating the grating drive arm with a stepper-motor-driven cam. The cam has a fast rise rate when moving from one of the 12 wavelengths to the next, and also maintains a constant radius so that a given wavelength is displayed to an accuracy of 0.2 Å at the exit slit. The transfer time from one wavelength to the next is 0.5 sec, and total scan cycle time is 32 sec. A cam-driven system gives accurate, reproducible wavelengths, and it requires only one point for wavelength calibration. After two years of operation on Nimbus-4, the BUV double monochromator has maintained a wavelength accuracy of better than 1 Å.

b. Electronics

The signal-processing electronics of the monochromator and photometer channels are virtually identical and only one channel will be described. The

nine decades of optical signal levels received at the photomultiplier are accommodated by a programmed high voltage power supply, a three-range electrometer, and a two-mode digital ratemeter. The photomultiplier is operated at two discrete gain states by automatically adjusting the high voltage power supply. In the low gain state only analog current signals are obtained, while in the high gain state pulse-count data are available in addition to the analog signals.

In the analog mode, the signal-processing channel consists of an electrometer, an automatic range sequencer, and a logarithmic analog-to-digital converter. The electrometer produces an output voltage which is proportional to the average input current.

The output voltage is sensed by an automatic range sequencer and is utilized to select any of the three feedback resistors and the two high voltage levels, hence controlling the system gain. Gain changes can occur every 200 milliseconds except during the automatic reference adjustment period. Possible gain states are 10^7, $2x10^9$ and $3x10^{10}$ volts/ampere in the low voltage state and 10^7 volts/ampere in the high voltage state.

The signal-processing channel in the pulse-counting mode consists of an electrometer (common to both analog and pulse-counting modes), a pulse amplifier/shaper, a single-channel pulse-height selector, and a digital ratemeter. In the pulse-counting mode the electrometer serves as a wide-band pulse

amplifier. The pulses from the electrometer are further amplified and appropriately shaped for input to the discriminators. The high and low level discriminators and an anticoincidence circuit form a single-channel analyzer. The low level discriminator removes noise, while the upper discriminator is utilized to compensate for radiation-induced pulses. The output pulses from the anticoincidence circuit are counted for the 1.8 second dwell time at each wavelength step.

4. OBSERVATIONS

A computer plot of the experiment data from one complete orbit is shown in Figure 3. The radiances found with the photometer and the 12 monochromator channels are given by the upper 12 lines in this plot. The units are ergs/cm^2 · sec · Å · ster and ergs/cm^2 · sec · Å for the atmospheric radiance and solar irradiance, respectively. The top of the ordinate scale is 10^2. From left to right the data record begins with earth radiance measurements in the northern hemisphere. Moving northward, the radiance decreases with increasing solar zenith angles. At the northern terminator the diffuser plate is deployed for two complete scans. Then the diffuser is stowed and the spacecraft moves toward satellite night. A residual signal due to sunlight reflected off the entrance horns drops abruptly with passage into satellite night. The daytime equatorial signal is about 100 times above the background; the nighttime background signal is about a factor of ten greater than the typical dark current observed in the prelaunch testing. The large nighttime increase in signal is due

to photomultiplier currents induced as the spacecraft passes through a portion of the South Atlantic anomaly of the Van Allen radiation belts. A global contour map of radiation-belt-induced dark-currents is shown in Figure 4. On the figure, the units when multiplied by 10^{-15} amperes are cathode current. A contour of 5×10^{-15} amperes is equivalent to 10 percent of the signal produced by the equatorial radiance at 2550 Å. Consequently, a significant part of the data reduction effort is directed towards establishing a dark-current correction to be applied to the observations.

Some evidence for secular changes in high-level ozone has been found. Atmospheric radiances in the vicinity of 2900 Å appear to have remained constant over a two-year time span, implying that ozone in the 30- to 40-kilometer region is quite stable.

At the shorter wavelengths, from the radiances increased during the same time period. This could imply that the high-level ozone distribution is decreasing with the decreasing phase of the eleven-year sunspot cycle. Nimbus-4 was launched a little more than one year after solar maximum of the current sunspot cycle. Similar observations of a decrease in atmospheric ozone in the upper stratosphere with declining solar activity have also been reported by Dutsch [2] from Umkehr data and by Paetzold [15, 16] from balloon data. A significant solar-cycle variation in the solar irradiance which dissociates O_2 in the upper stratosphere and lower mesosphere has been reported by Heath [5] from rocket and Nimbus-3 and Nimbus-4 satellite experiments.

The fundamental observation of the BUV experiment is the ultraviolet terrestrial albedo, which is defined as the ratio of earth radiance to the extraterrestrial solar irradiance, I/F_0. A typical equatorial albedo determination by the BUV experiment is shown in Figure 5. The crosses represent the equatorial albedo observed with the U.S.S.R. COSMOS satellites using a double monochromator in 1965 and 1966. The observations have been reported by Krasnopol'skiy [9], Iozenas [6], and Iozenas et al. [7, 8]. These measurements occurred at solar minimum of the last sunspot cycle. The agreement is excellent at 3000 A, however, the curves diverge as one goes to shorter wavelengths. This trend of increasing equatorial albedo with decreasing sunspot activity is the same as that observed with the BUV experiment. One cannot dismiss completely that it is an artifact due to instrumental scattered light, although the accumulation of experimental evidence would seem to indicate otherwise. Only the U.S.S.R. experiments on the COSMOS satellites and the BUV experiment on Nimbus-4 measured the extraterrestrial solar irradiance in conjunction with terrestrial atmospheric radiances. Others have had to rely on published values of the ultraviolet solar irradiance, which may introduce serious errors in the values for albedo if there is an eleven-year solar-cycle variation in the ultraviolet solar irradiance as reported by Heath [5].

Figure 6 is an example of total ozone above the 10 and 2.8 mb pressure levels displayed on northern and southern polar stereographic projections. Gaps in the data are the result of failure of an onboard tape recorder, of the

absence of a nearby tracking station to carry out satellite interrogation, or high dark-current backgrounds induced by the inner regions of the Van Allen radiation belts. Figure 7 is an example of derived total ozone for both hemispheres.

Prabhakara et al. [17] has derived global maps of total ozone from observations in the 9.6 micron band of O_3, utilizing the Infrared Interferometer Spectrometer (IRIS) experiment flown on Nimbus-3 and -4. An early comparison of inferred total ozone for the BUV and IRIS experiments on Nimbus-4 shown for a single daylight passage in Figure 8. The shipboard Dobson spectrophotometer measurements by White and Krueger [18] shown in this figure required 54 days, whereas the satellite observations were made in 54 minutes. The photometer channel at 3800 Å can be used to infer approximate Lambertian surface reflectivities at the wavelength pairs used in the derivation of total ozone. An investigation of this approximation from upward and downward spectrophotometric flux measurements have been made by Furukawa and Heath [4] from the NASA/Convair 990 research aircraft for the determination of surface reflectivities in the wavelength range of 3000 Å to 4800 Å. Until these results can be incorporated into the BUV analysis programs, an interim approach has been to evaluate an equivalent surface albedo which has been derived from a regression analysis between Dobson spectrophotometer "ground truth" measurements and the BUV data, for example, see Mateer, Heath, and Krueger [12]. In general, the standard errors of estimate between the BUV and Dobson derived ozone values are about 0.02 atm-cm. The satellite values appear to be

a little too low or a little too high, depending upon whether the total ozone is low or high respectively.

The basic BUV experiment data consist of unedited radiance data which are stored on archive tapes at the World Data Center A. Production of total ozone data and high-level ozone profiles continues as confidence in the validity of the data and analysis increases. Available data will include global atlases of total ozone, height distributions in the form of the amount above different pressure levels, and the basic atmospheric radiance data.

5. ACKNOWLEDGMENTS

The success of the BUV experiment and its continued operation after nearly three years in orbit are due in large part to efforts of the Beckman Instrument Corp. and the Analog Technology Corp. who built the experiment. These contributions are gratefully acknowledged.

REFERENCES

[1] G. P. Anderson et al., Satellite observations of the vertical ozone distribution in the upper stratosphere, Annales de. Geophysique, 25 (1969), 341-345.

[2] J. V. Dave and C. L. Mateer, A preliminary study of the possibility of estimating total atmospheric ozone from satellite measurements, J. Atmos. Sci., 24 (1967), 414-427.

[3] H. U. Dutsch, Atmospheric ozone and ultraviolet radiation, Climate of the Free Atmosphere, vol. 4 of World Survey of Climatology, Elsevier Publishing Co., 1969, 382-432.

[4] P. Furukawa and D. F. Heath (to be published).

[5] D. F. Heath, Space observations of the variability of solar irradiance in the near and far ultraviolet, J. Geophys. Res. (in press) (1973).

[6] V. A. Iozenas, Determining the vertical ozone distribution in the upper atmospheric layers from satellite measurements of ultraviolet solar radiation scattered by the earth's atmosphere, Geomag. Aeron., 8 (1968), 403-407.

[7] V. A. Iozenas et al., Studies of the earth's ozonosphere from satellites, Izv. Atmos. Oceanic Phys., 5 (1969), 77-82.

[8] V. A. Iozenas et al., An investigation of the planetary ozone distribution from satellite measurements of ultraviolet spectra, Izv. Atmos. Oceanic Phys., 5 (1969), 219-233.

[9] V.A. Krasnopol'skiy, The ultraviolet spectrum of solar radiation reflected by the terrestrial atmosphere and its use in determining the total content and vertical distribution of atmospheric ozone, Geomag. Aeron., 6 (1966), 236-242.

[10] A.J. Krueger, D.F. Heath, and C.L. Mateer, Variations in the stratospheric ozone field inferred from Nimbus Satellite observations, Pure and Applied Geophysics, vol. 19, 1973.

[11] C.L. Mateer, A Review of Some Aspects of Inferring the Ozone Profile by Inversions of Ultraviolet Radiance Measurement, in The Mathematics of Profile Inversion, edited by L. Colin, NASA TMX-62 (1972), pp. 2-25.

[12] C.L. Mateer, D.F. Heath, and A.J. Krueger, Estimation of total ozone from satellite measurements of backscattered ultraviolet earth radiance, J. Atmos. Sci. 28 (1971), 1307-1311.

[13] R.D. Rawcliffe and D.D. Elliott, Latitude distributions of ozone at high altitudes deduced from satellite measurement of the earth's radiance at 2840 A. J. Geophys. Res., 71 (1966), 5077-5089.

[14] S.F. Singer and R.C. Wentworth, A method for the determination of the vertical ozone distribution from a satellite, J. Geophys. Res., 62 (1957), 299-308.

[15] H.K. Paetzold, Variation of the vertical ozone profile over middle Europe from 1951 to 1968, Ann. Geophys., 25 (1969), 347-349.

[16] H. K. Paetzold, Secular variations of the atmospheric ozone layer cover middle Europe from 1951 to 1968, XV General Assembly, I. U. G. G., Moscow, 1971.

[17] C. Prabhakara, E. B. Rogers, and V. V. Salmonson, Remote sensing of the global distribution of total ozone and the inferred upper-tropospheric circulation from Nimbus IRIS experiment, Pure and Applied Geophysics, vol. 19, 1973.

[18] W. C. White and A. J. Krueger, Shipboard observations of total ozone from 30 N to 60 S, J. Atmos. Terr. Phys., 30 (1968), 1615-1622.

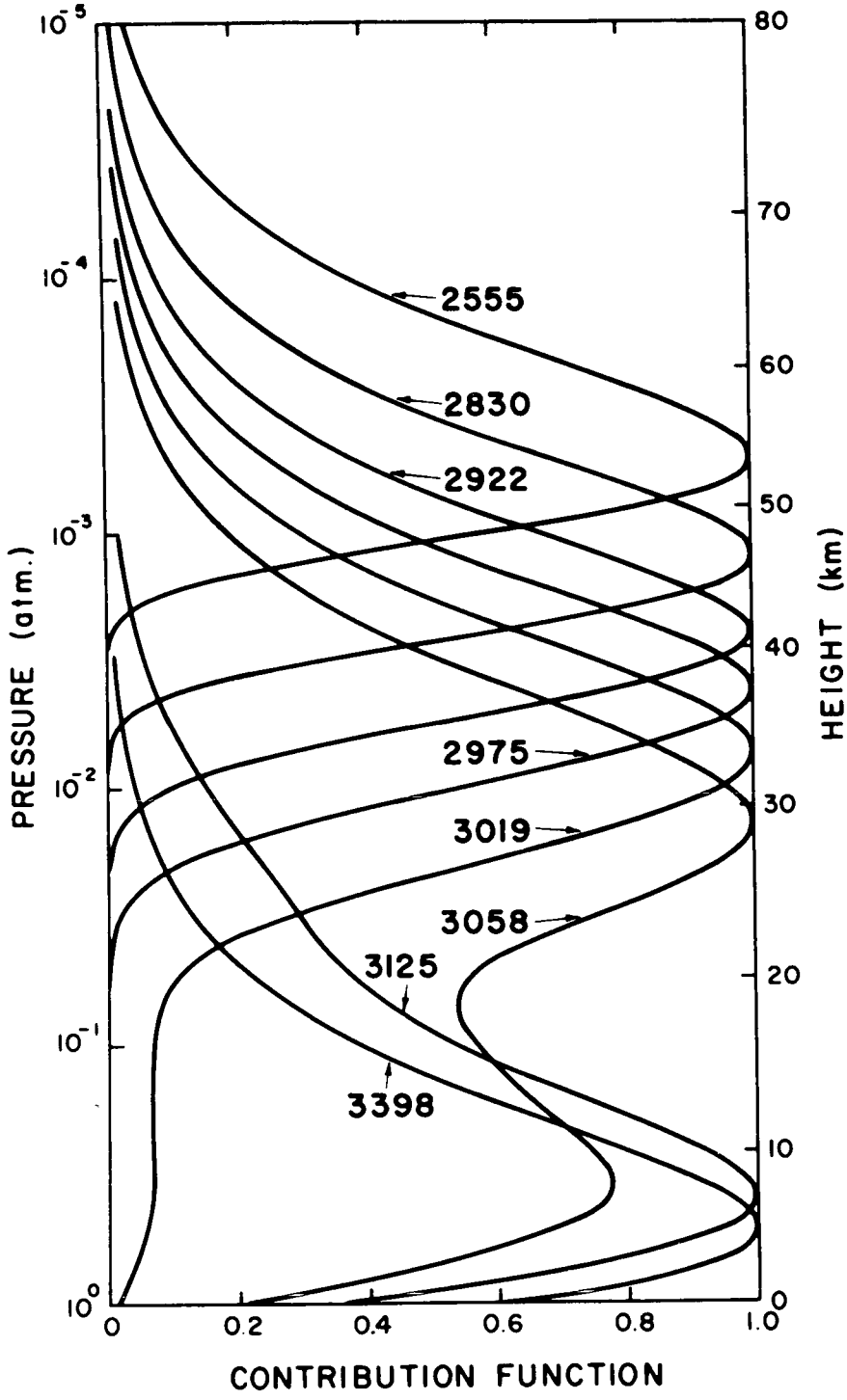

Figure 1. Effective scattering levels for solar radiation scattered in the nadir direction of the satellite for all orders of scattering; solar zenith angle = 60° and total ozone = 336 m atm-cm.

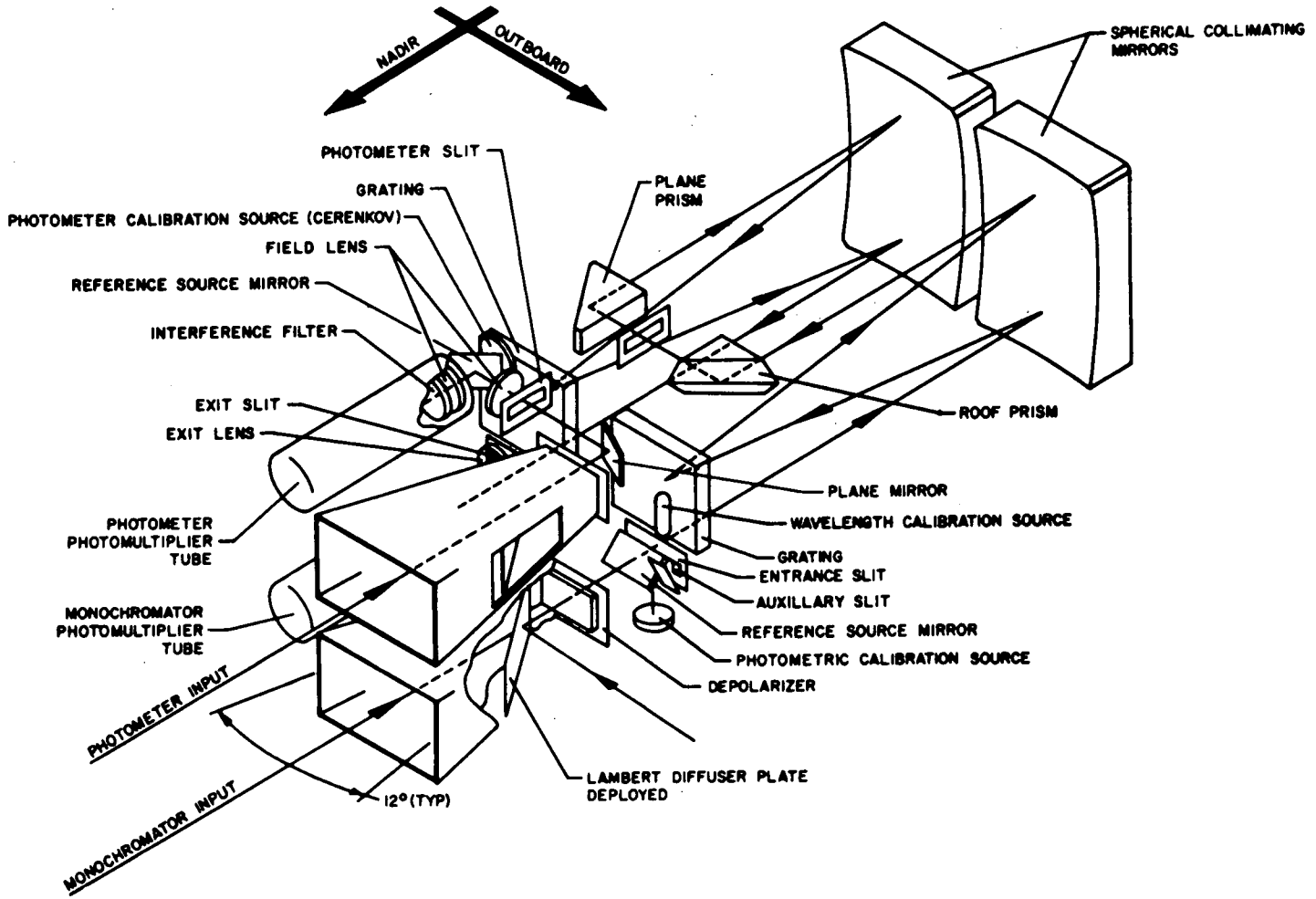

Figure 2. Optical path through the Nimbus-4 Backscatter Ultraviolet experiment.

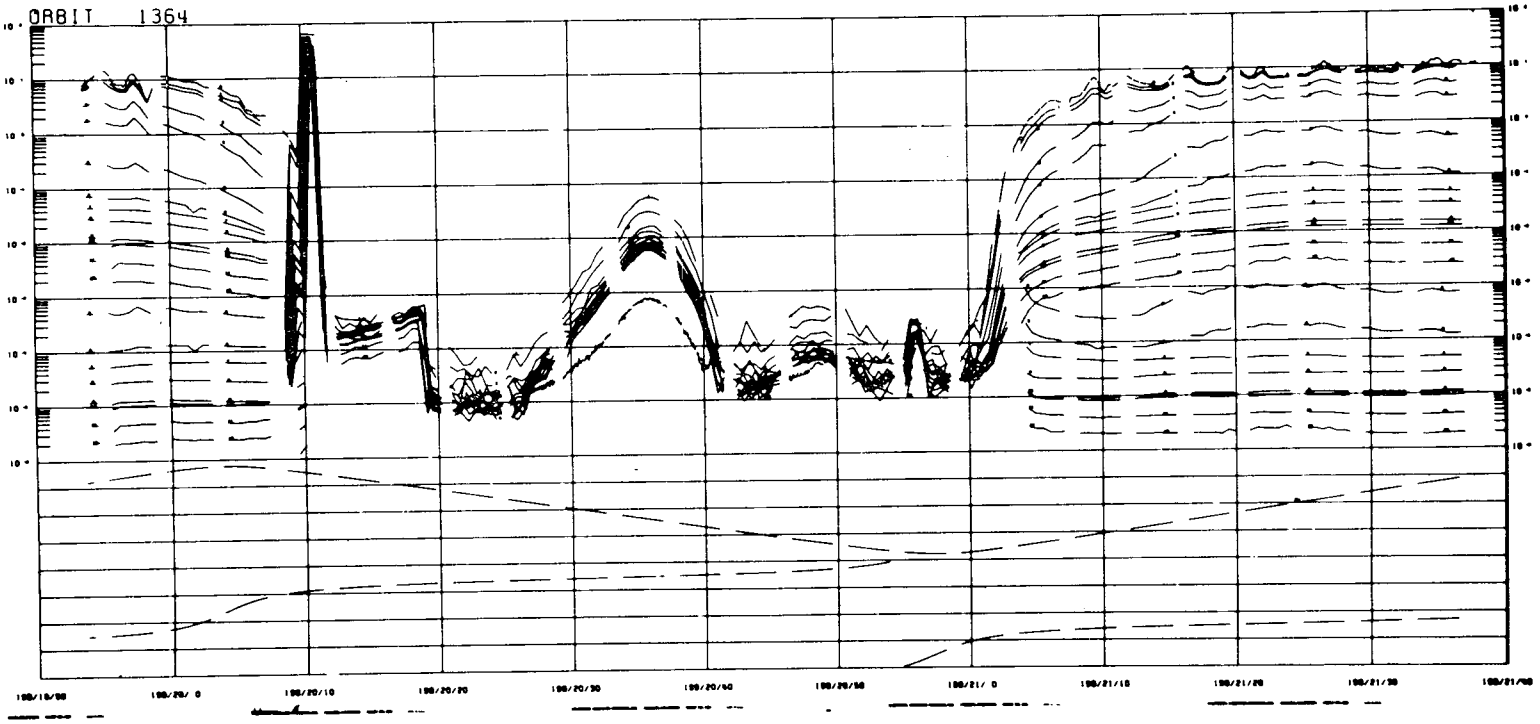

Figure 3. Computer plot of a typical orbit of BUV data.

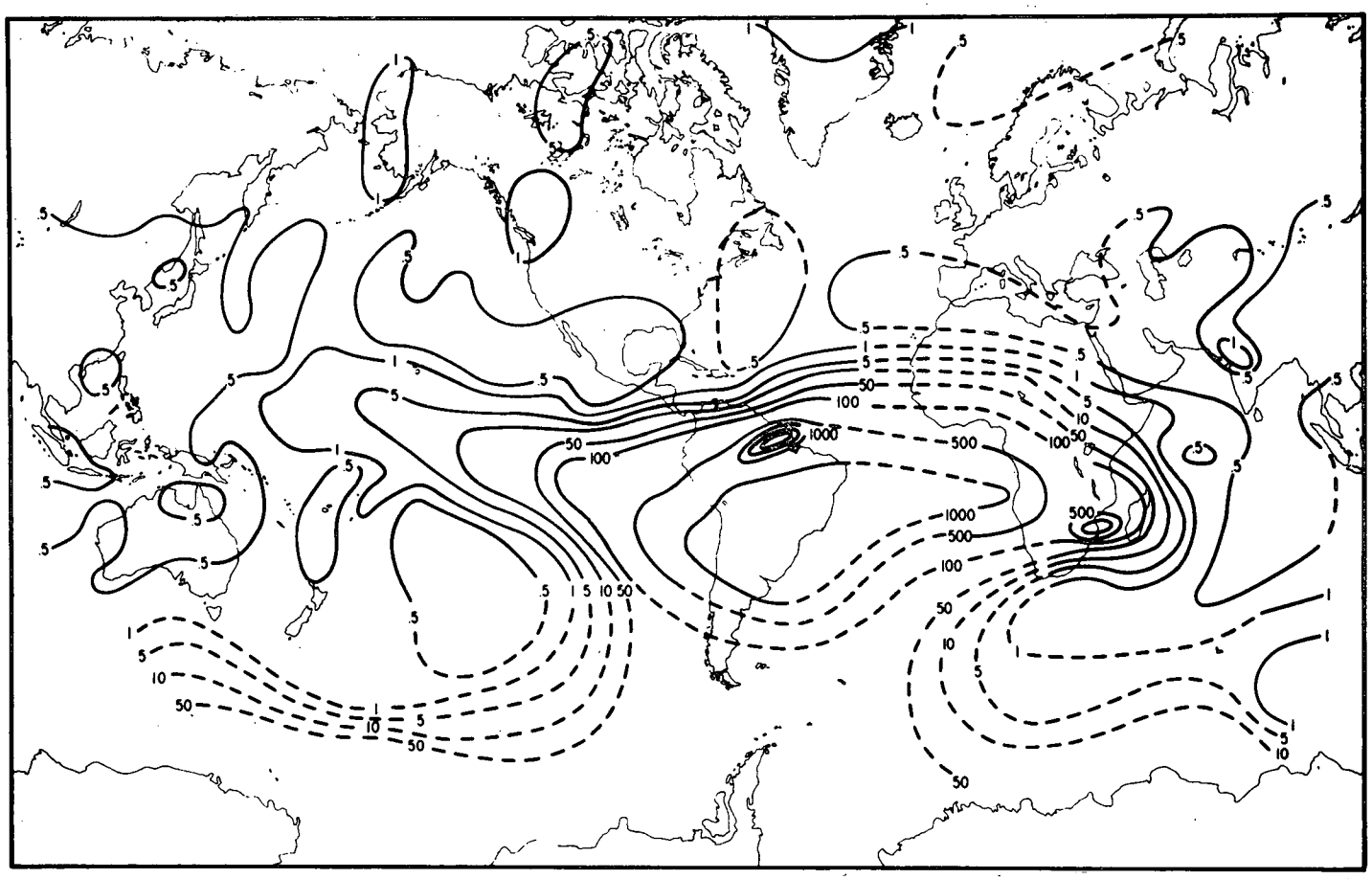

Figure 4. Geographical representation of Van Allen radiation-belt-induced dark-current signals. The units are for the monochromator photomultiplier cathode current when multiplied by 10^{-15} amperes.

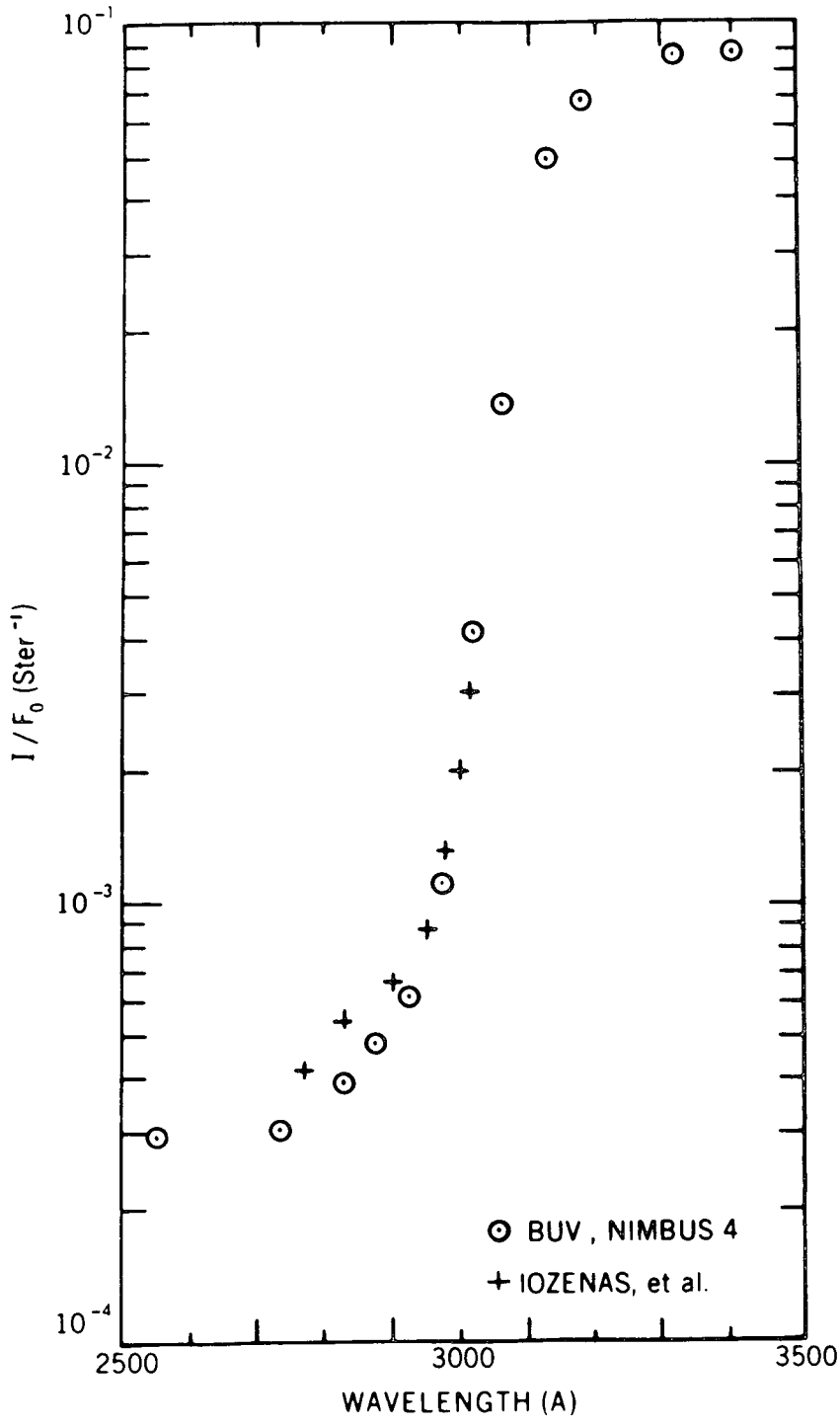

Figure 5. Comparison of equatorial albedo observed with the Nimbus-4 BUV experiment in 1970 and the U. S. S. R. experiments on the COSMOS satellite series in 1965 and 1966.

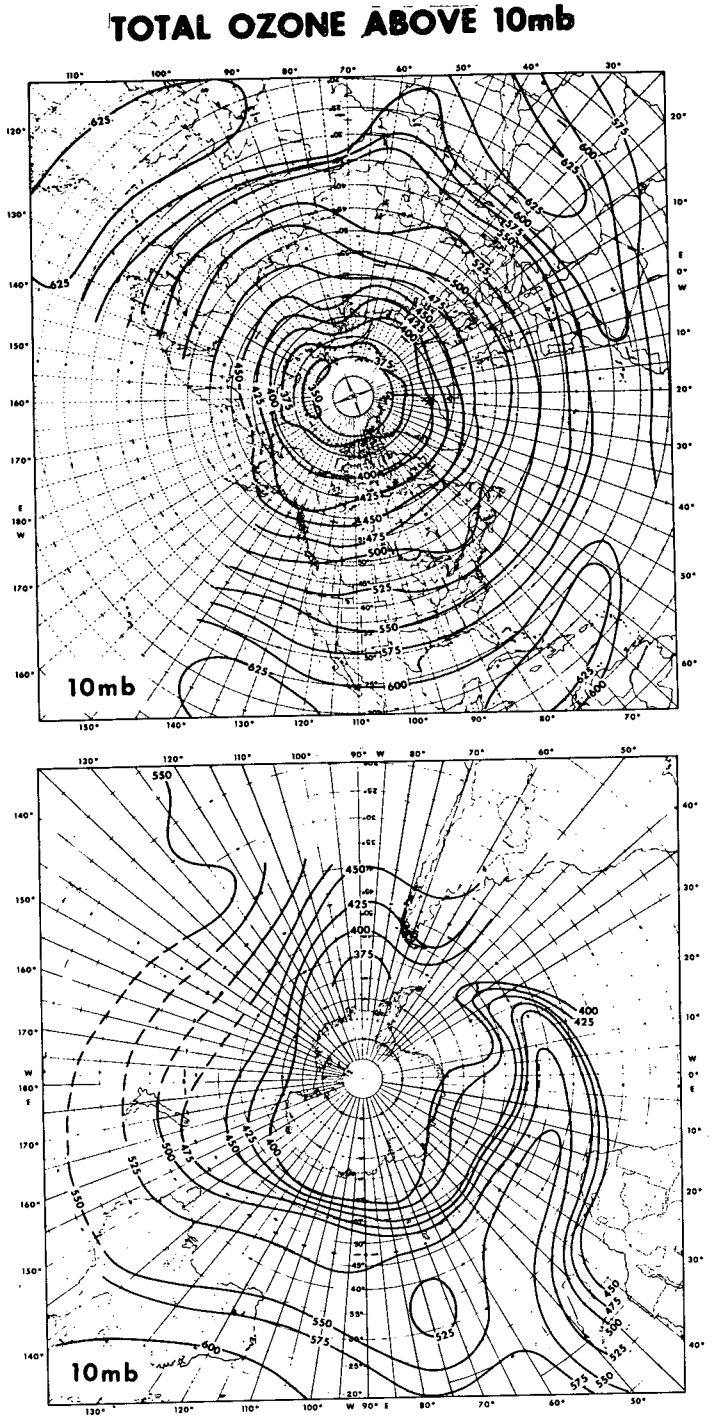

Figure 6. Examples of a global map of the amount of ozone above pressure levels 10 mb and 2.8 mb for the northern and southern hemispheres. (Sheet 1)

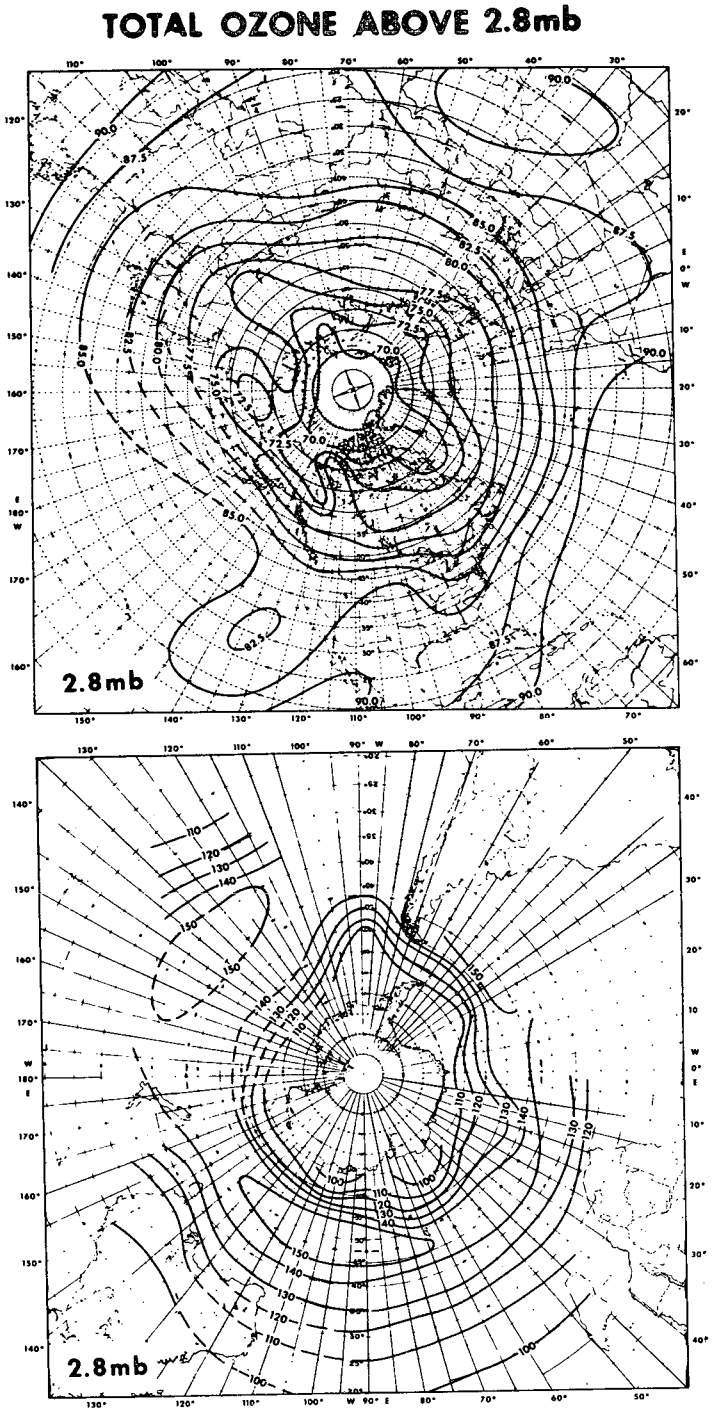

Figure 6. Examples of a global map of the amount of ozone above pressure levels 10 mb and 2.8 mb for the northern and southern hemispheres. (Sheet 2)

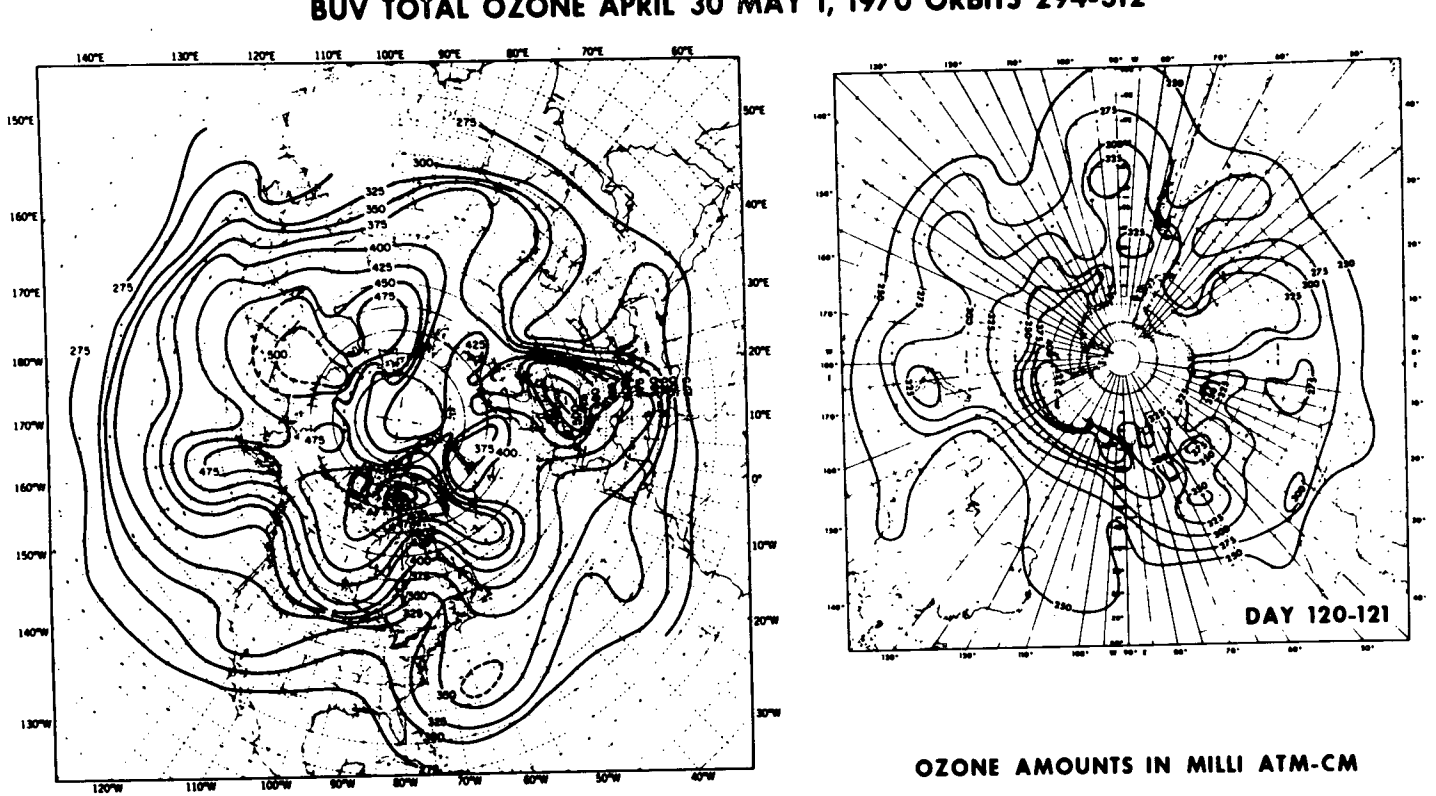

Figure 7. Global map of total ozone inferred from the Nimbus-4 BUV experiment.

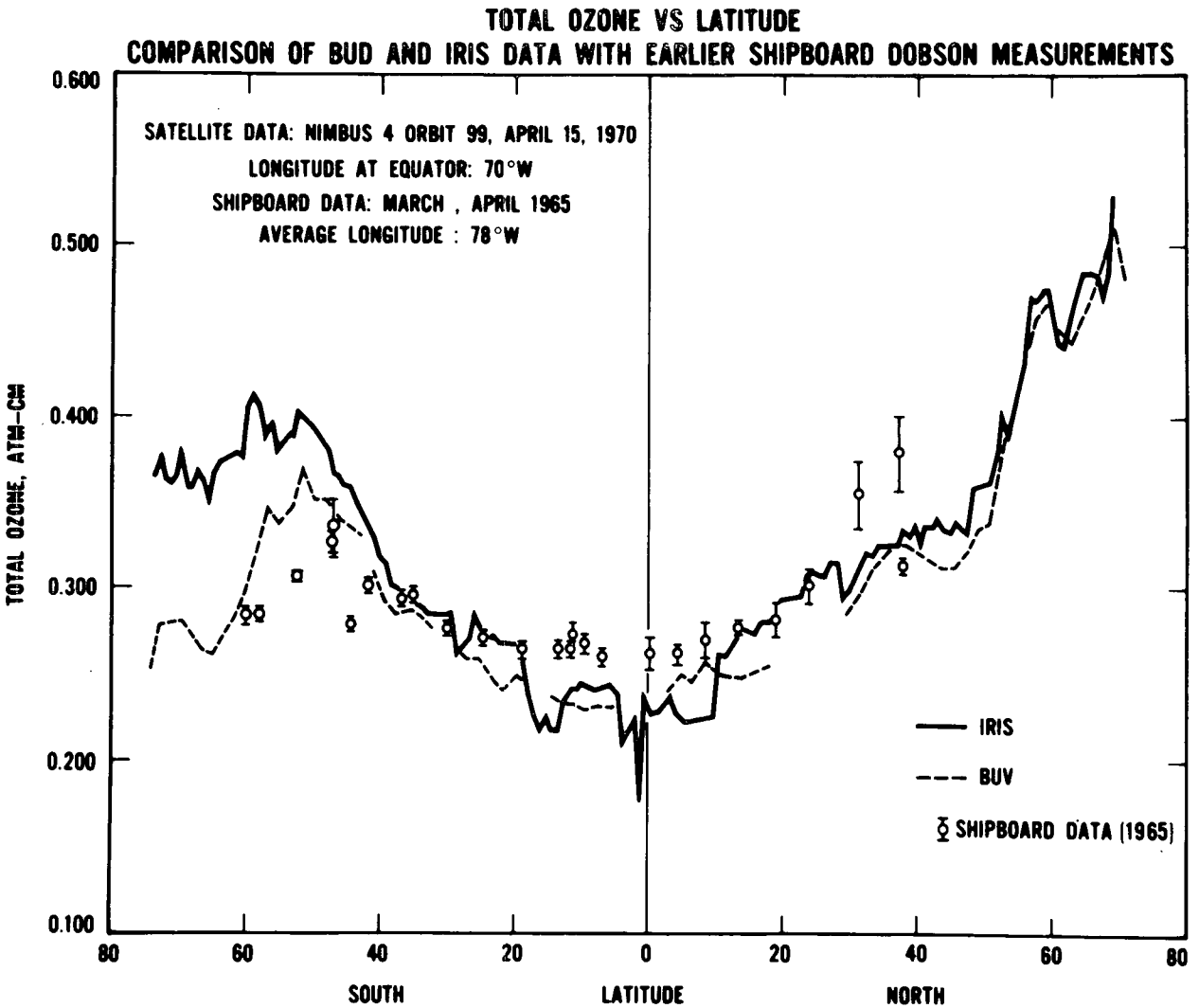

Figure 8. Comparison of total ozone along a daylight satellite pass derived from ultraviolet radiance (BUV), infrared radiance (IRIS), and earlier Dobson measurements from shipboard.